

# Synthesis and properties of 1,3,4-oxadiazole-containing bismaleimides with asymmetric structure and the copolymerized systems thereof with 4,4'-bismaleimidodiphenylmethane

 Lianlian Xia,<sup>a</sup> Xuejiao Zhai,<sup>a</sup> Xuhai Xiong<sup>b</sup> and Ping Chen<sup>\*ab</sup>

 Cite this: *RSC Adv.*, 2014, 4, 4646

Two novel bismaleimide monomers containing 1,3,4-oxadiazole and asymmetric structure, *i.e.*, 2-[4-(4-maleimidophenoxy)phenyl]-5-(4-maleimidophenyl)-1,3,4-oxadiazole (*p*-Mioxd) and 2-[3-(4-maleimidophenoxy)phenyl]-5-(4-maleimidophenyl)-1,3,4-oxadiazole (*m*-Mioxd), were designed and synthesized. The chemical structures of the monomers were confirmed using Fourier transform infrared spectroscopy (FTIR), <sup>1</sup>H NMR and <sup>13</sup>C NMR spectroscopy and elemental analysis. The thermal properties of the monomers were investigated by differential scanning calorimetry (DSC) and thermogravimetric analysis (TGA). The results indicate that the incorporation of the 1,3,4-oxadiazole and asymmetric structure could improve the solubility and processability of the BMI monomers and the thermal stability of the resins. Composites composed of glass cloth and 4,4'-bismaleimidodiphenylmethane (BMDM), which were modified with 2.5, 5 and 10 wt% *p*-Mioxd and *m*-Mioxd, respectively, were also prepared. The TGA and DMA results demonstrate that the resulting composites have excellent thermal stability with high residual weight percentage at 700 °C (>45%) and *T*<sub>g</sub> (>450 °C).

 Received 24th September 2013  
 Accepted 31st October 2013

DOI: 10.1039/c3ra45313h

[www.rsc.org/advances](http://www.rsc.org/advances)

## Introduction

Bismaleimides and thermoplastic polyimides are high-performance polymers for applications in elevated temperature operations for which conventional epoxy systems may not be sufficiently stable.<sup>1–3</sup> The fiber-reinforced composites based on BMI resins are widely employed in the aerospace industry and for electronic/electrical materials such as multilayer and printed circuit boards and insulators, due to their excellent thermal and mechanical properties.<sup>4–7</sup> Nonetheless, the ordinary BMIs with their rigid and symmetric molecular structure suffer from high melting temperature and poor solubility in common solvents, and the cured resins have inherent brittleness due to their high crosslinking density.<sup>4a</sup>

Various methods to enhance the toughness of BMI resins have been reported in the literature.<sup>8–12</sup> Among them, an effective method is modifying the chemical structure of the BMI monomers, and many efforts have been made to design and synthesize a number of new chain-extended BMI monomers, such as those containing phosphorus,<sup>13–15</sup> silicon,<sup>16a,17</sup> naphthalene,<sup>18a–c</sup> biphenylene,<sup>19</sup> dicyclopentadiene or dipentene,<sup>18d</sup> and fluorenyl cardo groups.<sup>20</sup> Aromatic poly(1,3,4-oxadiazole) is

a class of chemically resistant and thermally stable heterocyclic polymers with high glass transition temperatures (*T*<sub>g</sub>) and melting temperatures (*T*<sub>m</sub>).<sup>25</sup> Many kinds of thermally stable polymers based on 1,3,4-oxadiazoles have been synthesized and studied, such as polyamides,<sup>21,22</sup> poly(arylene ether)s,<sup>23a,b</sup> and polyimides.<sup>24</sup> Incorporating a 1,3,4-oxadiazole ring into the BMI skeletons in order to improve their properties without sacrificing their mechanical, electrical or thermal performance has received considerable attention during the last few decades. Several BMI monomers containing a 1,3,4-oxadiazole moiety have been reported in the literature.<sup>4b,16b,25</sup> However, those BMI monomers containing a 1,3,4-oxadiazole moiety had high melting temperatures (*T*<sub>m</sub>), and sharp curing exothermic peaks followed, which resulted in poor processability. Among them, a BMI monomer with an asymmetric structure had been synthesized in order to place the terminal double bonds of BMI in different chemical surroundings and improve the processability.<sup>4b</sup> Unfortunately, it just broadened the curing exothermic peak and the process window was still narrow.

In this paper, we reported the synthesis and characterization of two novel BMI monomers with asymmetric structure and a 1,3,4-oxadiazole moiety. The solubility and thermal properties of the monomers were investigated. The composites composed of glass cloth and 4,4'-bismaleimidodiphenylmethane (BMDM), which were modified with 2.5, 5 and 10 wt% *p*-Mioxd and *m*-Mioxd, respectively, were also prepared. Their thermal and mechanical properties were studied using TGA and DMA.

<sup>a</sup>State Key Laboratory of Fine Chemicals, School of Chemical Engineering, Dalian University of Technology, Dalian 116024, China. E-mail: chenping\_898@126.com

<sup>b</sup>Liaoning Key Laboratory of Advanced Polymer Matrix Composites Manufacturing Technology, Shenyang Aeronautics University, Shenyang 110136, China

## Results and discussion

### Synthesis and characterization of BMI monomers

The BMI monomers containing 1,3,4-oxadiazole (*i.e.*, *p*-Mioxd and *m*-Mioxd) were designed and synthesized following the route illustrated in Scheme 1. C-1 was synthesized according to the method reported previously.<sup>25</sup> C-2a and C-2b were achieved from the nucleophilic substitution reaction of *p*-chloronitrobenzene with *p*-Cresol and *m*-Cresol, respectively, which were oxidized by a  $\text{KMnO}_4/\text{OH}^-$  system to yield C-3a and C-3b with a total yield above 85%. The dinitro compounds (C-4a and C-4b) were prepared by cyclodehydration of C-1 with C-3a and C-3b, respectively, in the presence of PPA, and then reduced to diamine compounds by hydrazine with  $\text{FeCl}_3/\text{C}$  as a catalyst. The resultant diamines (*p*-DA and *m*-DA) reacted with maleic anhydride in acetone at ambient temperature to afford the corresponding bismaleamic acids, which were subjected to imidization in the presence of triethylamine, sodium acetate and acetic anhydride to yield *p*-Mioxd and *m*-Mioxd at an overall yield of 54.6% and 52.9%.

The chemical structures of *p*-Mioxd and *m*-Mioxd were confirmed by FTIR,  $^1\text{H}$  NMR,  $^{13}\text{C}$  NMR and elemental analysis. In the FTIR spectrum of the diamine compounds (*p*-DA and *m*-DA), there are both four absorption peaks in the 3200–3500  $\text{cm}^{-1}$  range as shown in Fig. 1, which is not consistent with the conventional diamines. Meanwhile, in the  $^1\text{H}$  NMR spectrum of *p*-DA and *m*-DA, different chemical shift values (5.94 and 5.08 ppm) and (5.96 and 5.08 ppm) for amino groups of *p*-DA and *m*-DA are observed, respectively (Fig. 2). This phenomenon may be attributed to the asymmetric molecular structure, which leads to the different reactivity of the two terminal amino groups in the diamines, *i.e.*, *p*-DA and *m*-DA.

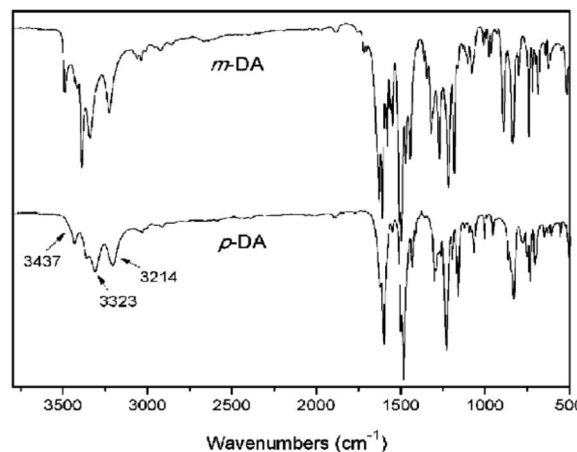
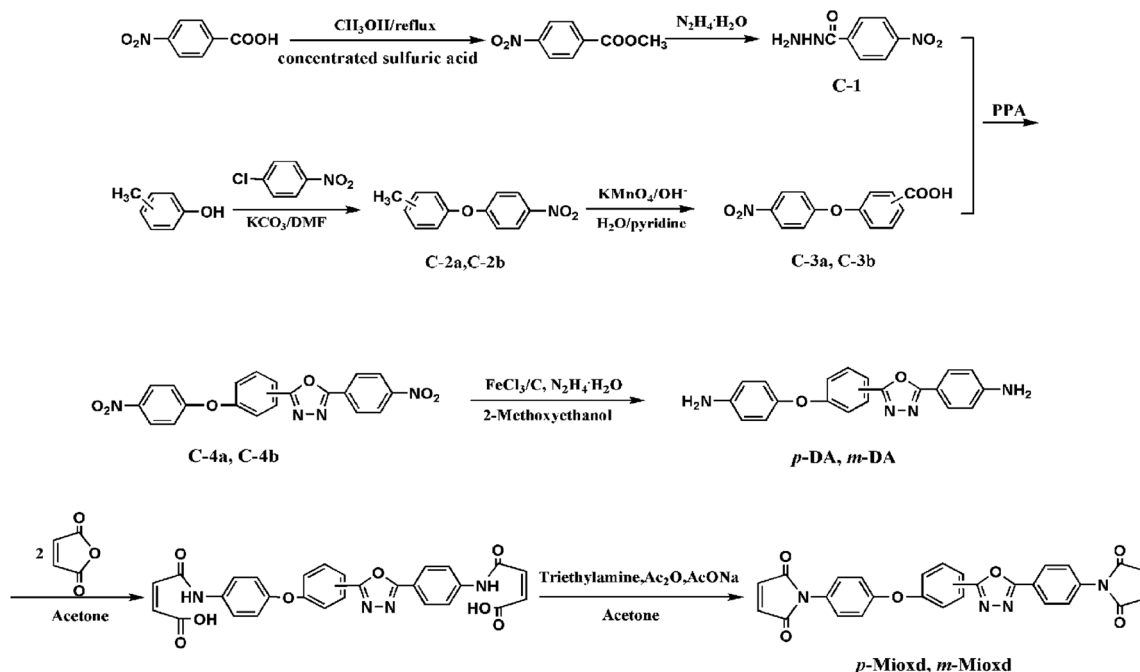


Fig. 1 The FTIR spectra of the diamine compounds.

Fig. 3 shows the typical FTIR for two BMI monomers (*p*-Mioxd and *m*-Mioxd), the absorption peaks, *i.e.* 1719 ( $\nu_{\text{C}=\text{O}}$  of maleimide), 1608 ( $\nu_{\text{C}=\text{N}}$  of 1,3,4-oxadiazole), 1397, 1150 ( $\nu_{\text{C}-\text{N}-\text{C}}$  of maleimide) and 691 ( $\nu_{\text{C}=\text{C}}$  of maleimide) confirm the structure of the two bismaleimides.<sup>16b</sup> The  $^1\text{H}$  NMR spectra of the two monomers with the assignments of all the protons are presented in Fig. 4; there are both two sharp singlet signals at 7.25, 7.20 ppm and 7.23, 7.20 ppm, which are assigned to the olefinic protons of two maleimide end groups. This confirms the  $\text{C}=\text{C}$  bonds of the two maleimide end groups may have different reactivities. The integral of each proton agrees well with the proposed structure. Fig. 5 shows the  $^{13}\text{C}$  NMR spectra of the two monomers; there are 18 and 20 singlet signals for *p*-Mioxd and *m*-Mioxd, respectively, in accordance with the number of non-equivalent carbon atoms.



Scheme 1 Synthetic route of the BMI monomers, *e.g.* *p*-Mioxd and *m*-Mioxd.

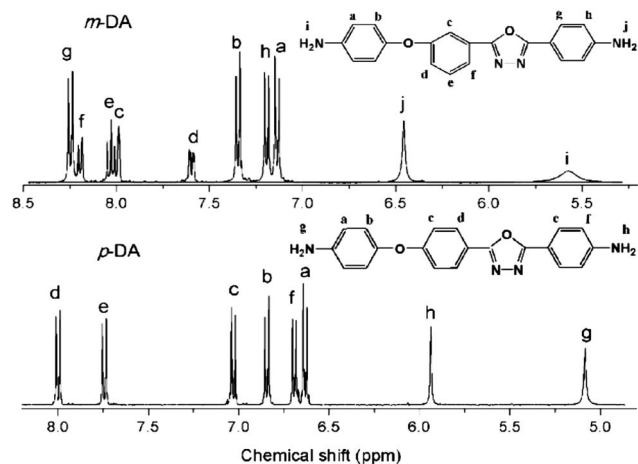


Fig. 2 The  $^1\text{H}$  NMR spectra of the diamine compounds.

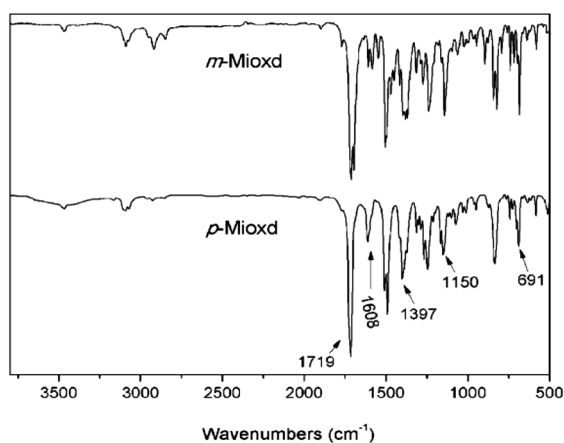


Fig. 3 The FTIR spectra of the BMI monomers.

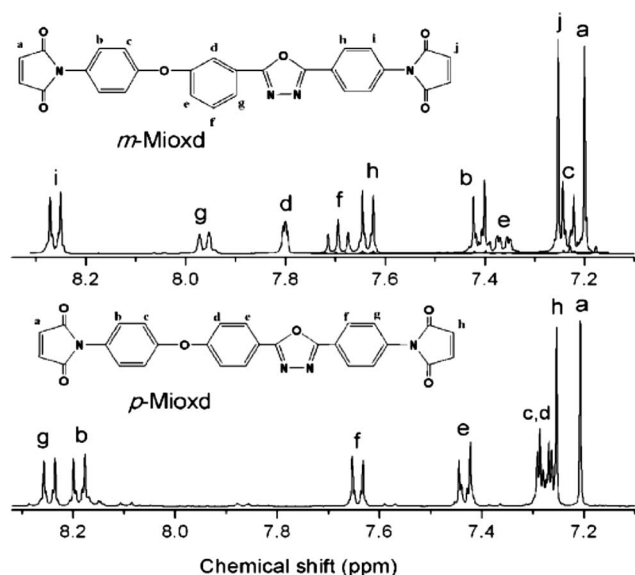


Fig. 4 The  $^1\text{H}$  NMR spectra of the BMI monomers.

## The solubility and thermal properties of BMI monomers

The solubilities of *p*-Mioxd and *m*-Mioxd were evaluated in various solvents, and the results are listed in Table 1. Both *p*-Mioxd and *m*-Mioxd are soluble in a variety of organic solvents, such as chloroform, dichloromethane, tetrahydrofuran, dimethyl-sulfoxide, *N,N*-dimethylformamide, and *N*-methyl-2-pyrrolidone. However, *p*-Mioxd exhibits poorer solubility in comparison with *m*-Mioxd. The presumed explanation is that the *meta*-substitution in *m*-Mioxd lowers the symmetry of the molecular chains, thus reducing the crystallinity and improving the solubility.

The curing behavior of *p*-Mioxd and *m*-Mioxd was investigated by DSC at  $10\text{ K min}^{-1}$ . As shown in Fig. 6, *p*-Mioxd exhibits a peculiar curve showing two endothermic peaks at  $174.5\text{ }^\circ\text{C}$  and  $247.1\text{ }^\circ\text{C}$ , and two exothermic peaks at  $180.4\text{ }^\circ\text{C}$  and  $271.3\text{ }^\circ\text{C}$ , which is different from common BMI monomers, which exhibit only one endothermic peak due to melting, and one exothermic peak assigned to the thermally curing process. A similar phenomenon had been reported previously, and it was thought that the first and the second exothermic transitions should be correlated to the polymerization reaction between olefinic bonds.<sup>16b</sup> But the  $E_a$  values of the first of *p*-Mioxd were calculated to be  $50.96\text{ kJ mol}^{-1}$  and  $49.54\text{ kJ mol}^{-1}$ , according to the Kissinger equation and the Ozawa equation, which were lower than the other reported BMI monomers (about  $100\text{ kJ mol}^{-1}$ ).<sup>18a</sup> In comparison, the *p*-Mioxd sample was first heated at a rate of  $10\text{ K min}^{-1}$  to  $200\text{ }^\circ\text{C}$ , kept for 30 min, and cooled down to  $150\text{ }^\circ\text{C}$ , then heated to  $350\text{ }^\circ\text{C}$  at the same rate. The obtained DSC curve was shown in Fig. 6, where we could only observe the second exothermic transitions. To investigate further, the *m*-Mioxd, *p*-Mioxd and the *p*-Mioxd after heat treatment at  $200\text{ }^\circ\text{C}$  for 30 min were analyzed by a polarized optical microscope as shown in Fig. 7, where we can see only one crystal form in (a) and (c), and two crystal forms in (b), so we think that the first heat transition should be ascribed to the transformation of the crystal form. The *m*-Mioxd has one endothermic peak at  $206.3\text{ }^\circ\text{C}$  attributed to melting, and one exothermic peak at  $283.1\text{ }^\circ\text{C}$  assigned to the curing process. The values of the curing characteristics for *p*-Mioxd and *m*-Mioxd were reported in Table 2. Compared with *p*-Mioxd undergoing a rapid thermal curing upon melting, *m*-Mioxd has a lower melting point, and a broader processing window. This may be responsible for the *meta*-substitution in the structure of *m*-Mioxd, which lowers the symmetry of molecular chain, thus reducing the crystallinity and melting temperature.

The thermal properties of *p*-Mioxd and *m*-Mioxd were investigated by TGA at  $20\text{ K min}^{-1}$  in nitrogen. As shown in Fig. 8, both display excellent thermal stability with temperatures for 5% weight loss at  $504.2\text{ }^\circ\text{C}$  and  $498.7\text{ }^\circ\text{C}$ . The residual weights of *p*-Mioxd and *m*-Mioxd at  $700\text{ }^\circ\text{C}$  are both above 60%.

The activation energies ( $E_a$ ) of the curing reaction of *p*-Mioxd and *m*-Mioxd were calculated from DSC measurement by employing the Kissinger equation and the Ozawa equation.<sup>1b,26a</sup>

Kissinger equation:

$$d\left[\ln\left(\beta/T_p^2\right)\right]/d(1/T_p) = -E_a/R$$

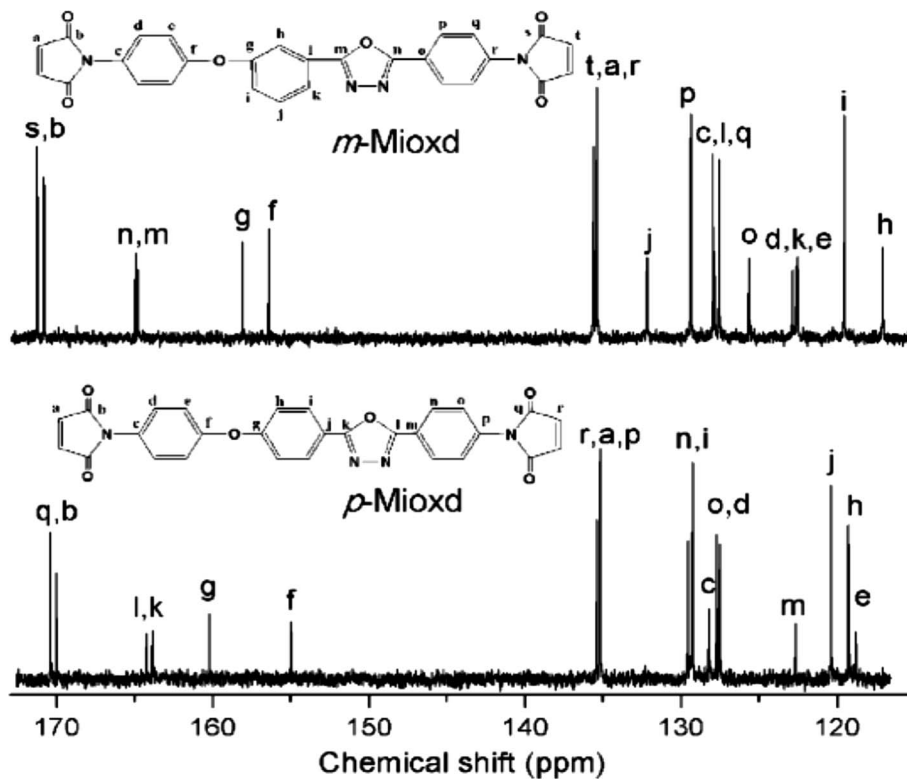


Fig. 5 The  $^{13}\text{C}$  NMR spectra of the BMI monomers.

Ozawa equation:

$$d(\log \beta)/d(1/T_p) = -0.4567E_a/R$$

where  $E_a$  is the activation energy,  $R$  is the gas constant,  $\beta$  is the heating rate, and  $T_p$  is the exothermic transition temperature of the corresponding  $\beta$ . To estimate the activation energy ( $E_a$ ), a series of dynamic DSC scans were conducted at heating rates of 2.5, 5, 10, 15 and 20  $\text{K min}^{-1}$ , and the results were shown in Table 3. On the basis of the Kissinger equation and the Ozawa equation, the kinetic plots were drawn in Fig. 9 and the  $E_a$  values were obtained from the slope of the graph of  $\ln(\beta/T_p^2)$  versus  $1/T_p$  and of  $\ln \beta$  versus  $1/T_p$ . The  $E_a$  values of the first heat transition of  $p$ -Mioxd were calculated to be 50.96  $\text{kJ mol}^{-1}$  and 49.54  $\text{kJ mol}^{-1}$  according to the Kissinger equation and the Ozawa equation, which were lower than the other reported BMI monomers (about 100  $\text{kJ mol}^{-1}$ ).<sup>18a</sup> The  $E_a$  values of the second curing process of  $p$ -Mioxd and  $m$ -Mioxd, *i.e.* 124.7  $\text{kJ mol}^{-1}$ , 129.0  $\text{kJ mol}^{-1}$  and 125.4  $\text{kJ mol}^{-1}$ , 128.7  $\text{kJ mol}^{-1}$ , respectively, were very comparable with typical BMI.

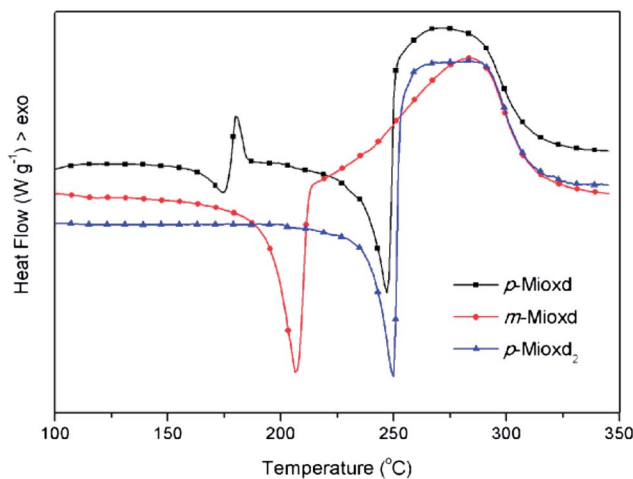


Fig. 6 The DSC curves of  $p$ -Mioxd and  $m$ -Mioxd at a heating rate of 10  $\text{K min}^{-1}$  in nitrogen, and  $p$ -Mioxd<sub>2</sub>: first heated at a rate of 10  $\text{K min}^{-1}$  to 200  $^{\circ}\text{C}$ , kept for 30 min, cooled down to 150  $^{\circ}\text{C}$  and then heated again to 350  $^{\circ}\text{C}$  at the same rate.

Table 1 The solubility of BMI monomers

	Ethanol	Acetone	Toluene	DCM	Chloroform	THF	DMF	DMSO	NMP
$p$ -Mioxd	–	+	+	+	++	+	++	++	++
$m$ -Mioxd	–	+	+	++	++	++	++	++	++

<sup>a</sup> '+' = soluble ( $>10 \text{ mg mL}^{-1}$ ), '++' = soluble under heating, '–' = insoluble. DCM, dichloromethane; THF, tetrahydrofuran; DMF,  $N,N$ -dimethylformamide; DMSO, dimethylsulfoxide; NMP,  $N$ -methyl-2-pyrrolidinone.

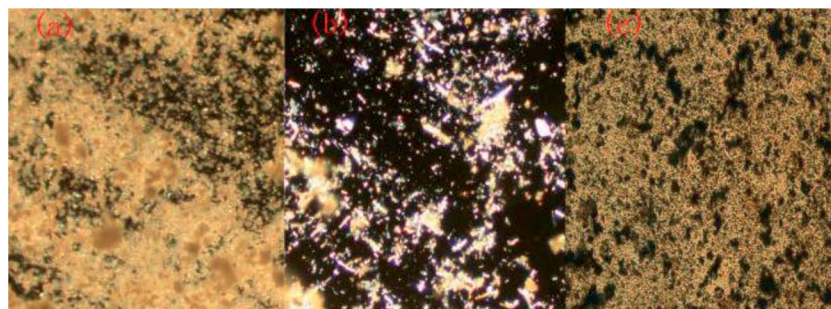


Fig. 7 The polarized optical microscopy photograph of BMI monomers. (a) *m*-Mioxd, (b) *p*-Mioxd, and (c) *p*-Mioxd after heat treatment at 200 °C for 30 min.

### Thermal and mechanical properties of composites composited with BMI mixtures and glass cloth

Both *p*-Mioxd and *m*-Mioxd were found to be difficult for processing due to the high melting points and narrow processing window. Since mixtures of BMI monomers have been successfully employed to decrease the melting and curing temperature,<sup>26b,27</sup> thus BMI monomer mixtures based on *p*-Mioxd/MBMI and *m*-Mioxd/MBMI with various percentages (2.5, 5, 10 wt%) were prepared in our study. The DSC investigation of the BMI monomer mixtures is shown in Fig. 10 and Table 2, where we can see that all samples display a sharp melting transition at around 160 °C and a broad exothermic transition assigned to the curing process. The  $T_m$  of *p*-Mioxd/MBMI systems is found to increase from 161.5 °C to 162.4 °C with the weight percentage of *p*-Mioxd increasing from 2.5% to 5%, but decrease to 160.5 °C when the percentage is 10%.  $T_p$  represents a similar trend, which increases from 293.3 °C to 293.7 °C and then decreases to 292.1 °C.  $T_m$  and  $T_p$  of the *m*-Mioxd/MBMI systems display a contrary trend compared with the *p*-Mioxd/MBMI systems, which first decrease and then increase with the addition of *p*-Mioxd. The results indicate that the processing properties of *p*-Mioxd and *m*-Mioxd could be improved using mixtures of them with MBMI. All

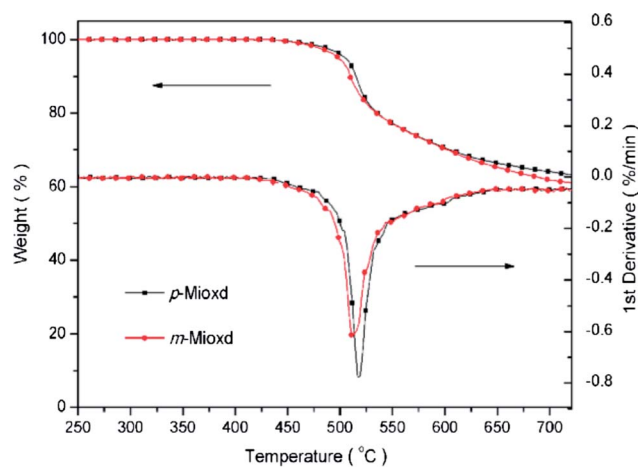


Fig. 8 The TGA curves of the resins based on *p*-Mioxd and *m*-Mioxd at a heating rate of 20 K min<sup>-1</sup> in nitrogen.

mixtures have a lower  $T_m$  of about 160 °C and a wider processing window, defined as  $T_i - T_m$ , of about 90 °C.

The thermal stability of the BMI mixtures with various percentages were investigated by TGA (Fig. 11 and Table 4). It is

Table 2 The DSC cure characteristics of BMI monomers and their mixtures with MBMI

Code	$T_m^a$ (°C)	$T_i^b$ (°C)	$T_p^c$ (°C)	$T_f^d$ (°C)	$T_i - T_m^e$ (°C)	$\Delta H$ (J g <sup>-1</sup> )	
<b>BMI monomers</b>							
MBMI	160.3	177.8	219.5	245.7	17.5	60.9	
<i>p</i> -Mioxd	247.1	248.3	271.3	306.2	—	189.3	
<i>m</i> -Mioxd	206.3	237.9	283.1	308.5	31.6	109.1	
<i>p</i> -Mioxd <sub>2</sub>	174.5	—	180.4	—	—	6.8	
<b><i>p</i>-Mioxd/MBMI (wt%)</b>							
2.5%	<i>p</i> -Mioxd-2.5	161.7	243.6	293.3	335.9	88.1	115.8
5%	<i>p</i> -Mioxd-5	162.4	253.2	293.7	332.7	90.8	90.3
10%	<i>p</i> -Mioxd-10	160.5	248.3	292.1	332.5	87.8	90.8
<b><i>m</i>-Mioxd/MBMI (wt%)</b>							
2.5%	<i>m</i> -Mioxd-2.5	162.2	247.6	294.4	339.7	85.4	121.3
5%	<i>m</i> -Mioxd-5	158.4	249.6	289.7	343.5	91.2	150.5
10%	<i>m</i> -Mioxd-10	159.7	251.2	293.9	344.7	91.5	108.9

<sup>a</sup> The melting transition temperature. <sup>b</sup> The initial curing temperature. <sup>c</sup> The exothermic transition temperature. <sup>d</sup> The final curing temperature. <sup>e</sup> The processing window.

**Table 3** The DSC analysis of *p*-Mioxd, *m*-Mioxd monomers at different heating rates

Heating rate $\beta$ (K min <sup>-1</sup> )	$T_{p1}^a$ (°C)	$T_{p2}^b$ (°C)	$T_{p3}^c$ (°C)
2.5	174.6	251.2	251.8
5	177.9	262.1	264.4
10	180.4	276.3	283.1
15	182.1	288.1	290.4
20	182.9	296.8	296.8

<sup>a</sup> The first exothermic transition temperature of *p*-Mioxd. <sup>b</sup> The second exothermic transition temperature of *p*-Mioxd. <sup>c</sup> The exothermic transition temperature of *m*-Mioxd.

observed that the temperatures required for 5% and 10% weight loss of the *p*-Mioxd/MBMI systems are found to increase from 511.2 °C to 519.4 °C and from 512.7 °C to 521.7 °C, respectively, and the residual weight percentage at 700 °C apparently increased from 48.5% to 58.3% with increasing concentration of *p*-Mioxd. The temperatures required for 5% and 10% weight loss of the *m*-Mioxd/MBMI systems float at around 516.5 °C and 519.5 °C, respectively, while the residual weight percentage at 700 °C increased from 54.8% to 62.2% with increasing concentration of *m*-Mioxd, as shown in Table 4. The results indicate that incorporation of *p*-Mioxd and *m*-Mioxd improves the thermal stability and enhances the residual weight percentage at 700 °C of pure BMI monomers, due to the thermal stable aromatic heterocyclic and 1,3,4-oxadiazole structure of *p*-Mioxd and *m*-Mioxd.

The thermal mechanical properties are the most important properties of high-performance materials for advanced composites. In our study, DMA was employed to assess these properties of the composites composed of *p*-Mioxd/MBMI or *m*-Mioxd/MBMI with glass cloth. Fig. 12 and 13 show the temperature dependence of storage modulus ( $E'$ ) and loss tangent ( $\tan \delta$ ) for the prepared composites, respectively. As shown in Fig. 12(a) and (b), the  $E'$  values for the composites composed of modified resins in the glassy region are found to be decreased; this may be caused by the chain extension of *p*-Mioxd and *m*-Mioxd compared with MBMI, which hinders the tight packing of the molecular chain. The  $E'$  values increase from 6.06 GPa to 9.57 GPa with increasing percentage concentration of *p*-Mioxd, while *m*-Mioxd modified resins display a

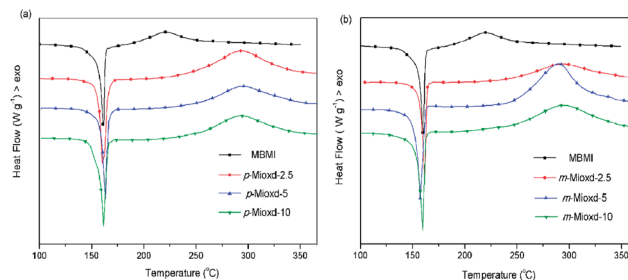


**Fig. 10** The DSC curves of the BMI monomer mixtures at a heating rate of 10 K min<sup>-1</sup> in nitrogen. (a) *p*-Mioxd/MBMI systems, (b) *m*-Mioxd/MBMI systems.

contrary trend, decreasing from 7.82 GPa to 6.95 GPa. This unusual phenomenon may be attributed to the *para*-substitution in the structure of *p*-Mioxd, which resulted in the tight packing of molecules. From Fig. 13(a) and (b), it is observed that the  $T_g$  of composites composed of *p*-Mioxd/MBMI or *m*-Mioxd/MBMI with glass cloth are above 450 °C, except for the *p*-Mioxd-10 system, indicating the excellent thermal stability of the resulting composites.

## Experimental

### Materials

*p*-Nitrobenzoic acid, *p*-chloronitrobenzene, *p*-Cresol and *m*-Cresol were supplied by Sinopharm Chemical Reagent Co. (Shanghai, China), and used as received. 4,4'-Bismaleimidodiphenylmethane (BMDM) was purchased from Yantai Hengxing Chemical Industrial Technologic Company and purified by column chromatography on silica gel. The glass cloth were supplied by Anhui Danfeng Group. Acetone and triethylamine were purified by distillation under reduced pressure over calcium hydride. Other chemical reagents were purchased from various commercial sources and used directly.

### Measurements

Fourier transform infrared (FTIR) spectra (KBr) were recorded on a Nicolet-20DXB IR spectrophotometer at 4 cm<sup>-1</sup> resolution and signal-averaged over 32 scans. Samples were prepared by

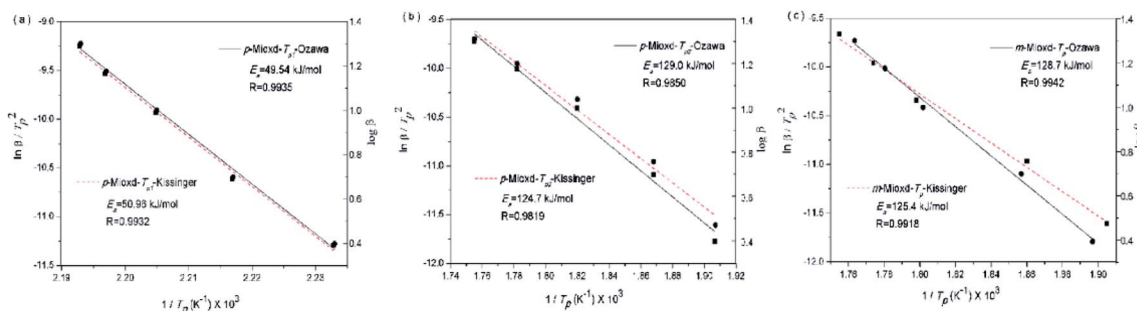


**Fig. 9** The kinetic plots of BMI monomers based on Ozawa equation and Kissinger equation, (a) first heat transition of *p*-Mioxd, (b) curing process of *p*-Mioxd, and (c) curing process of *m*-Mioxd.

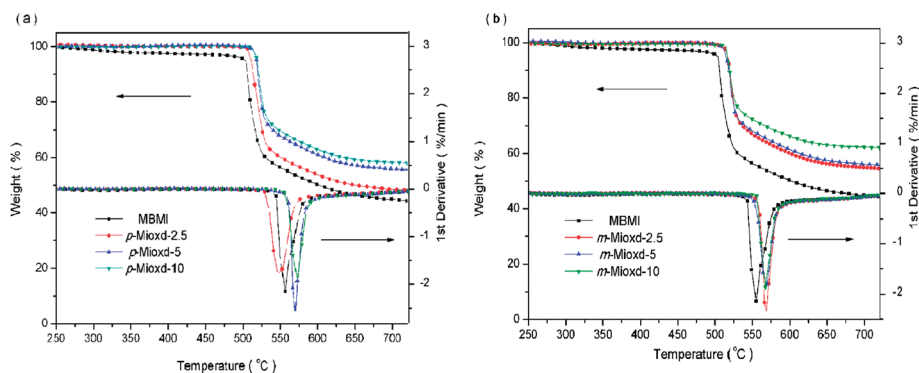


Fig. 11 The TGA curves of the BMI monomer mixtures at a heating rate of  $20 \text{ K min}^{-1}$  in nitrogen. (a) *p*-Mioxd/MBMI systems and (b) *m*-Mioxd/MBMI systems.

Table 4 TGA analysis of BMI monomers and their mixtures with MBMI

Sample	$T_{5\%}^a$ ( $^{\circ}\text{C}$ )	$T_{10\%}^b$ ( $^{\circ}\text{C}$ )	$T_{\text{max}}^c$ ( $^{\circ}\text{C}$ )	R.W. <sup>d</sup> (%)
MBMI	502.2	505.6	509.1	44.9
<i>p</i> -Mioxd	504.2	514.5	517.9	64.0
<i>m</i> -Mioxd	498.7	508.1	511.3	61.7
<i>p</i> -Mioxd-2.5	511.2	512.7	515.8	48.5
<i>p</i> -Mioxd-5	518.1	520.9	521.8	55.8
<i>p</i> -Mioxd-10	519.3	521.7	523.2	58.3
<i>m</i> -Mioxd-2.5	516.4	519.5	520.9	54.8
<i>m</i> -Mioxd-5	514.8	517.7	521.8	56.1
<i>m</i> -Mioxd-10	516.5	519.2	519.6	62.2

<sup>a</sup> The temperature at 5% weight loss. <sup>b</sup> The temperature at 10% weight loss. <sup>c</sup> The temperature corresponding to the maximum rate of weight loss. <sup>d</sup> The residual weight percentage at  $700^{\circ}\text{C}$ .

dispersing the material in KBr and compressing the mixtures to form disks.

$^1\text{H}$  NMR and  $^{13}\text{C}$  NMR were recorded on a Varian INOVA 400 MHz NMR spectrometer, using tetramethylsilane (TMS) as an internal reference. Chemical shifts ( $\delta$ ) were reported in ppm.

Elemental analysis was recorded using an Elemental Vario EL III instrument.

Differential scanning calorimetry (DSC) measurements were conducted with an NETZSCH DSC 204 instrument. About 6–9

mg samples were used at a heating rate of  $10 \text{ K min}^{-1}$  under a flow of nitrogen ( $20 \text{ mL min}^{-1}$ ).

Polarized optical microscopy graphs were recorded by Nikon OPTIPHOT2-POL.

Thermogravimetric analysis (TGA) was performed on a Perkin-Elmer TGA-7 thermal analyzer and all samples (around 6 mg) were heated from 25 to  $750^{\circ}\text{C}$  at a rate of  $20 \text{ K min}^{-1}$ , under a purified nitrogen flow rate of  $60 \text{ mL min}^{-1}$ .

Dynamic mechanical analysis (DMA) was done using a TA Instruments Q800 DMA with an amplitude of  $20 \mu\text{m}$ , driving frequency of 1.0 Hz and a temperature ramp rate of  $3 \text{ K min}^{-1}$  in a nitrogen atmosphere. The specimens were cut to dimensions of  $30 \text{ mm} \times 6 \text{ mm} \times 2 \text{ mm}$  for the single cantilever mode.

## Monomer synthesis

**Synthesis of 4-nitrobenzhydrazide (C-1).** 4-Nitrobenzhydrazide was synthesized according to the method reported previously at a yield of 95%.<sup>26a</sup> FTIR (KBr;  $\text{cm}^{-1}$ ):  $\nu = 3332, 3276$  ( $-\text{NH}-, -\text{NH}_2$ ),  $1647$  ( $-\text{C}=\text{O}$ ),  $1506, 1340$  ( $-\text{NO}_2$ ).  $^1\text{H}$  NMR (400 MHz;  $\text{CDCl}_3$ ):  $\delta = 8.30$  (d,  $J = 8.89 \text{ Hz}$ , 2H, Ar-H),  $8.05$  (d,  $J = 8.89 \text{ Hz}$ , 2H, Ar-H),  $10.14$  (s, 1H,  $-\text{NH}$ ),  $4.7$  (s, 2H,  $-\text{NH}_2$ ).

**Synthesis of 4-methyl-4'-nitrodiphenyl ether (C-2a) and 3-methyl-4'-nitrodiphenyl ether (C-2b).** *p*-Cresol (27.6 mL, 0.26 mol), anhydrous potassium carbonate (41.4 g, 0.3 mol), and dry

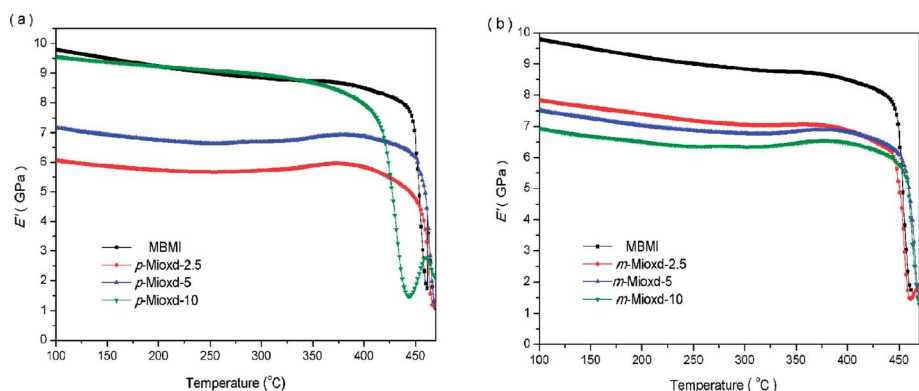


Fig. 12 The storage modulus for various composites. (a) Composites based on *p*-Mioxd/MBMI and (b) composites based on *m*-Mioxd/MBMI.

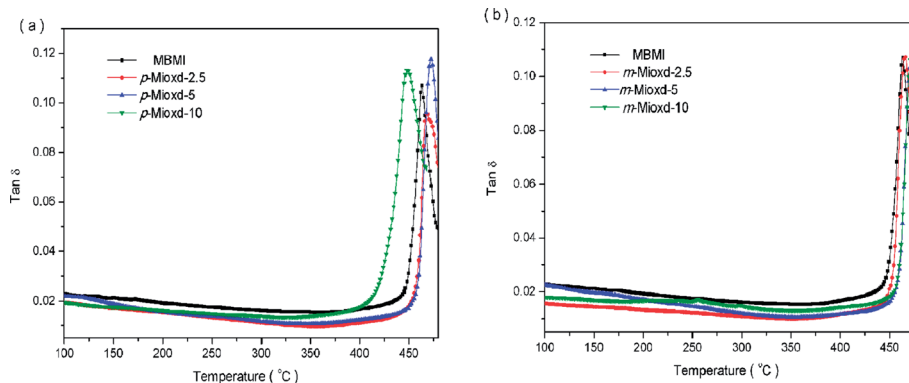


Fig. 13 The damping factor ( $\tan \delta$ ) for various composites. (a) Composites based on *p*-Mioxd/MBMI and (b) composites based on *m*-Mioxd/MBMI.

dimethyl-formamide (DMF, 150 mL) were placed into a 500 mL three-necked flask. The mixture was heated to 120 °C and stirred for 2 h, then a solution of *p*-chloronitrobenzene (41.8 g, 0.25 mol) in DMF (150 mL) was added dropwise over 1 h. After the addition, the reaction mixture was heated for another 10 h, and then separated by suction filtration. The resulting yellowish solid was precipitated by pouring the cooled filtrate into ice-cold water with constantly stirring. The crude C-2a was collected by filtration, washed thoroughly with distilled water and dried in an oven. The product was purified by column chromatography on silica gel (petroleum ether/dichloromethane), (54.37 g, yield 91%). FTIR (KBr;  $\text{cm}^{-1}$ ):  $\nu = 1506, 1344$  ( $-\text{NO}_2$ ), 1248, 1110 (Ar-O-Ar).  $^1\text{H NMR}$  (400 MHz;  $\text{CDCl}_3$ ):  $\delta = 8.19$  (d,  $J = 9.2$  Hz, 2H, Ar-H), 7.23 (d,  $J = 8.3$  Hz, 2H, Ar-H), 7.02–6.97 (m, 4H, Ar-H), 2.38 (s, 3H,  $-\text{CH}_3$ ).

C-2b was synthesized using an analogous method as described for C-2a, (yield: 92%). FTIR (KBr;  $\text{cm}^{-1}$ ):  $\nu = 2923, 2951$  ( $-\text{CH}_3$ ), 1501, 1345 ( $-\text{NO}_2$ ), 1250, 1108 (Ar-O-Ar).  $^1\text{H NMR}$  (400 MHz;  $\text{CDCl}_3$ ):  $\delta = 8.20$  (d,  $J = 9.10$  Hz, 2H, Ar-H), 7.30 (t, 1H, Ar-H), 7.26 (s, 1H, Ar-H), 7.07 (d, 1H, Ar-H), 7.01 (d,  $J = 9.10$  Hz, 2H, Ar-H), 6.89 (d, 1H, Ar-H), 2.38 (s, 3H,  $-\text{CH}_3$ ).

**Synthesis of 4-(4-nitrophenoxy) benzoic acid (C-3a) and 3-(4-nitrophenoxy) benzoic acid (C-3b).** C-2a (11.95 g, 0.05 mol), sodium hydroxide (10 g, 0.25 mol), distilled water (200 mL) and pyridine (100 mL) were placed into a 500 mL three-necked flask. The mixture was then heated to 100 °C, then potassium permanganate ( $\text{KMnO}_4$ , 39.5 g, 0.25 mol) was added three times over 0.5 h. After the addition, the reaction mixture was refluxed for 9 h until the potassium permanganate faded, and was then separated by suction filtration. The resulting white solid was precipitated by adding 20 mL concentrated sulfuric acid into the cooled filtrate under constant stirring. The C-3a was collected by filtration, washed thoroughly with distilled water and dried in an oven (12.3 g, yield 95%). FTIR (KBr;  $\text{cm}^{-1}$ ):  $\nu = 2500$ –3300 ( $-\text{COOH}$ ), 1685 ( $-\text{C}=\text{O}$ ), 1507, 1347 ( $-\text{NO}_2$ ), 1237, 1110 (Ar-O-Ar).  $^1\text{H NMR}$  (400 MHz;  $d$ -DMSO):  $\delta = 12.95$  (s, 1H,  $-\text{COOH}$ ), 8.30 (d,  $J = 8.9$  Hz, 2H, Ar-H), 8.03 (d,  $J = 8.41$  Hz, 2H, Ar-H), 7.25–7.27 (m, 4H, Ar-H).

C-3b was synthesized using an analogous method as described for C-3a (yield: 93%). FTIR (KBr;  $\text{cm}^{-1}$ ):  $\nu = 2500$ –3300

( $-\text{COOH}$ ), 1692 ( $-\text{C}=\text{O}$ ), 1504, 1346 ( $-\text{NO}_2$ ), 1251, 1110 (Ar-O-Ar).  $^1\text{H NMR}$  (400 MHz;  $d$ -DMSO):  $\delta = 13.46$  (s, 1H,  $-\text{COOH}$ ), 8.28 (d,  $J = 9.2$  Hz, 2H, Ar-H), 7.86 (d, 1H, Ar-H), 7.66 (s, 1H, Ar-H), 7.63 (t, 1H, Ar-H), 7.48 (d, 1H, Ar-H), 7.20 (d,  $J = 9.2$  Hz, 2H, Ar-H).

**Synthesis of 2-[4-(4-nitrophenoxy)phenyl]-5-(4-nitrophenyl)-1,3,4-oxadiazole (C-4a) and 2-[3-(4-nitrophenoxy)phenyl]-5-(4-nitrophenyl)-1,3,4-oxadiazole (C-4b).** C-1 (19.9 g, 0.11 mol), C-3a (25.9 g, 0.1 mol), polyphosphoric acid (PPA; 400 g) were placed into a flask, and then stirred to form a solution at 120 °C for 6 h. After cooling down to room temperature, the reaction mixture was poured into distilled water with stirring. The solid precipitate was filtered, washed with distilled water and subsequently with the dilute solution of sodium hydroxide, and finally dried in an oven (33.9 g, yield 84%). FTIR (KBr;  $\text{cm}^{-1}$ ):  $\nu = 1506, 1344$  ( $-\text{NO}_2$ ), 1250, 1114 (Ar-O-Ar), 1610 ( $\text{C}=\text{N}$ ), 968 ( $\text{C}-\text{O}-\text{C}$ ).  $^1\text{H NMR}$  (400 MHz;  $d$ -DMSO):  $\delta = 8.47$  (d,  $J = 8.84$  Hz, 2H, Ar-H), 8.40 (d,  $J = 8.84$  Hz, 2H, Ar-H), 8.32 (d,  $J = 9.15$  Hz, 2H, Ar-H), 8.27 (d,  $J = 8.63$  Hz, 2H, Ar-H), 7.44 (d,  $J = 8.63$  Hz, 2H, Ar-H), 7.31 (d,  $J = 9.15$  Hz, 2H, Ar-H).

C-4b was synthesized using an analogous method as described for C-4a (yield: 86%). FTIR (KBr;  $\text{cm}^{-1}$ ):  $\nu = 1509, 1347$  ( $-\text{NO}_2$ ), 1248, 1106 (Ar-O-Ar), 1606 ( $\text{C}=\text{N}$ ), 965 ( $\text{C}-\text{O}-\text{C}$ ).  $^1\text{H NMR}$  (400 MHz;  $d$ -DMSO):  $\delta = 8.43$  (d, 4H, Ar-H), 8.30 (d,  $J = 9.10$  Hz, 2H, Ar-H), 8.10 (d, 1H, Ar-H), 7.97 (s, 1H, Ar-H), 7.78 (t, 1H, Ar-H), 7.51 (d, 1H, Ar-H), 7.26 (d,  $J = 9.10$  Hz, 2H, Ar-H).

**Synthesis of 2-[4-(4-aminophenoxy)phenyl]-5-(4-aminophenyl)-1,3,4-oxadiazole (*p*-DA) and 2-[3-(4-aminophenoxy)phenyl]-5-(4-aminophenyl)-1,3,4-oxadiazole (*m*-DA).** C-4a (12.1 g, 0.03 mol), activated charcoal (8 g),  $\text{FeCl}_3$  (0.5 g), and 2-methoxyethanol (150 mL) were placed into a 250 mL three-necked flask. The reaction mixture was heated to 110 °C with stirring, and then 85% hydrazine monohydrate (25 mL) was added dropwise over 1 h. After the addition, the mixture was heated for another 10 h under a nitrogen atmosphere, and then separated by suction filtration. The resulting white solid was precipitated by pouring the cooled filtrate into ice-cold water under constant stirring. The precipitate was collected by filtration, dried and purified using ethanol (9.18 g, yield 89%). FTIR (KBr;  $\text{cm}^{-1}$ ):  $\nu = 3437, 3372, 3323, 3214$  ( $-\text{NH}_2$ ), 1236, 1067 (Ar-O-Ar), 1606 ( $\text{C}=\text{N}$ ), 960 ( $\text{C}-\text{O}-\text{C}$ ).  $^1\text{H NMR}$  (400 MHz;  $d$ -DMSO):

$\delta = 8.0$  (d,  $J = 8.93$  Hz, 2H, Ar-H), 7.74 (d,  $J = 8.69$  Hz, 2H, Ar-H), 7.03 (d,  $J = 8.93$  Hz, 2H, Ar-H), 6.84 (d,  $J = 8.76$  Hz, 2H, Ar-H), 6.69 (d,  $J = 8.69$  Hz, 2H, Ar-H), 6.63 (d,  $J = 8.76$  Hz, 2H, Ar-H), 5.94 (s, 2H,  $-\text{NH}_2$ ), 5.08 (s, 2H,  $-\text{NH}_2$ ).

*m*-DA was synthesized using an analogous method as described for *p*-DA (yield: 87%). FTIR (KBr;  $\text{cm}^{-1}$ ):  $\nu = 3470$ , 3383, 3329, 3220 ( $-\text{NH}_2$ ), 1213, 1068 (Ar-O-Ar), 1605 (C=N), 959 (C-O-C).  $^1\text{H}$  NMR (400 MHz; *d*-DMSO):  $\delta = 7.75$  (d,  $J = 8.7$  Hz, 2H, Ar-H), 7.7 (d, 1H, Ar-H), 7.53 (t, 1H, Ar-H), 7.49 (s, 1H, Ar-H), 7.10 (d, 1H, Ar-H), 6.85 (d,  $J = 8.8$  Hz, 2H, Ar-H), 6.70 (d,  $J = 8.7$  Hz, 2H, Ar-H), 6.64 (d,  $J = 8.8$  Hz, 2H, Ar-H), 5.96 (s, 2H,  $-\text{NH}_2$ ), 5.08 (s, 2H,  $-\text{NH}_2$ ).

**Synthesis of 2-[4-(4-maleimidophenoxy)phenyl]-5-(4-maleimidophenyl)-1,3,4-oxadiazole (*p*-Mioxd) and 2-[3-(4-maleimidophenoxy)phenyl]-5-(4-maleimido-phenyl)-1,3,4-oxadiazole (*m*-Mioxd).** C-5a (10.32 g, 0.03 mol), acetone (100 mL) were placed into a 250 mL three-necked flask, and stirred at room temperature. Thereafter a solution of maleic anhydride (6.17 g, 0.063 mol) in acetone (80 mL) was added into the reaction mixture dropwise. The suspension turned into a clear solution after the addition, and was stirred for another 9 h. The *N,N*-bismaleamic acid precipitated out, and was separated by suction filtration, washed with acetone to remove remain maleic anhydride and dried. A 250 mL three-necked flask was charged with acetone (150 mL), *N,N*-bismaleamic acid (10.8 g, 0.02 mol), triethylamine (1.2 mL) and sodium acetate (0.02 g). The reaction mixture was heated and refluxed until the suspension turned into a clear solution. Then acetic anhydride (5 mL) was added dropwise, and reflux was continued for an additional 6 h. The resulting solid was precipitated by pouring the reaction solution into ice-cold water with constant stirring. The precipitate was collected by filtration, washed with sodium bicarbonate until it was free from acetic acid, then finally washed with water and dried *in vacuo*, (15.1 g, yield 89%). FTIR (KBr;  $\text{cm}^{-1}$ ):  $\nu = 1720$  (C=O), 1611 (C=N), 1400, 1156 (C-N-C), 1266, 1072 (Ar-O-Ar), 956 (C-O-C), 691 (C=C).  $^1\text{H}$  NMR (400 MHz; *d*-DMSO):  $\delta = 8.25$  (d,  $J = 8.70$  Hz, 2H, Ar-H), 8.19 (d, 2H, Ar-H), 7.64 (d,  $J = 8.70$  Hz, 2H, Ar-H), 7.43 (d, 2H, Ar-H), 7.29 (d, 2H, Ar-H), 7.27 (d, 2H, Ar-H), 7.25 (s, 2H, C=C-H), 7.20 (s, 2H, C=C-H).  $^{13}\text{C}$  NMR (100 MHz; *d*-DMSO):  $\delta = 170.42$ , 170.04, 164.26, 163.97, 160.23, 154.99, 135.38, 135.18, 135.13, 129.57, 129.27, 128.23, 127.71, 127.51, 122.67, 120.39, 119.28, 118.82. Elemental analysis: (found: C, 66.59; H, 3.15; N, 11.23.  $\text{C}_{28}\text{H}_{16}\text{O}_6\text{N}_4$  requires C, 66.67; H, 3.17; N, 11.11%).

*m*-Mioxd was synthesized using an analogous method as described for *p*-Mioxd (yield 87%). FTIR (KBr;  $\text{cm}^{-1}$ ):  $\nu = 1713$  (C=O), 1615 (C=N), 1389, 1147 (C-N-C), 1247, 1065 (Ar-O-Ar), 956 (C-O-C), 689 (C=C).  $^1\text{H}$  NMR (400 MHz; *d*-DMSO):  $\delta = 8.26$  (d,  $J = 8.7$  Hz, 2H, Ar-H), 7.96 (d, 1H, Ar-H), 7.80 (s, 1H, Ar-H), 7.69 (t, 1H, Ar-H), 7.63 (d,  $J = 8.7$  Hz, 2H, Ar-H), 7.41 (d,  $J = 8.9$  Hz, 2H, Ar-H), 7.36 (d, 1H, Ar-H), 7.26 (s, 2H, C=C-H), 7.23 (d,  $J = 8.9$  Hz, 2H, Ar-H), 7.20 (s, 2H, C=C-H).  $^{13}\text{C}$  NMR (100 MHz; *d*-DMSO):  $\delta = 170.44$ , 170.02, 164.21, 164.05, 157.50, 155.86, 135.38, 135.25, 135.16, 132.02, 129.26, 127.86, 127.75, 127.47, 125.61, 122.87, 122.59, 122.51, 119.59, 117.16. Elemental analysis: (found: C, C, 66.62; H, 3.14; N, 11.18.  $\text{C}_{28}\text{H}_{16}\text{O}_6\text{N}_4$  requires C, 66.67; H, 3.17; N, 11.11%).

## Preparation of the composites composited with BMI mixtures and glass cloth

BMI monomer mixtures, *i.e.* *p*-Mioxd/MBMI or *m*-Mioxd/MBMI (2.5, 5, 10 wt%) was dissolved in DMF at a concentration of 0.5 g  $\text{mL}^{-1}$ , A glass cloth was impregnated with the solution for 24 h, and then hung vertically and dried at 80 °C *in vacuo*. The preregs were cut into pieces with dimensions 35 mm  $\times$  6.5 mm, stacked to a proper height, put between two steel sheets in a hydraulic press and cured following the regime: 180 °C for 4 h, 290 °C for 6 h, 300 °C for 2 h. The weight percentage of the resin in the final composites was determined to be around 40%.

## Conclusions

Two novel bismaleimide monomers containing 1,3,4-oxadiazole and asymmetric structure, *i.e.* *p*-Mioxd and *m*-Mioxd, were designed and synthesized, and both monomers had good solubility in common organic solvents. DSC investigations indicated that *p*-Mioxd had two exothermic transitions, which related to the transformation of the crystal form and the thermal curing of *p*-Mioxd, whereas *m*-Mioxd had only one exothermic transition related to the thermal curing of *m*-Mioxd. TGA investigations showed that the temperature for 5% and 10% weight loss was 504.2 °C, 514.5 °C for *p*-Mioxd and 498.7 °C, 508.1 °C for *m*-Mioxd, respectively. The residual weight percentages at 700 °C are all above 60%. The TGA results reveal that the *p*-Mioxd/MBMI systems and *m*-Mioxd/MBMI systems had excellent thermal stability with 10% weight loss above 510 °C and residual weight percentage at 700 °C in range 48–62%. The thermal mechanical properties of composites composed of *p*-Mioxd/MBMI or *m*-Mioxd/MBMI with glass cloth were obtained by DMA. The results showed a high storage modulus (>6.5 GPa) and  $T_g$  (>450 °C), indicating the excellent thermal stability of the resulting composites.

## Acknowledgements

The authors are grateful to the donors of the National Defense 12th 5-year program Fundamental Research Program (no. A3520110001), Liaoning Excellent Talents in University (no. LR2013002) and the National Natural Science Foundation of China (Grant No.51303107) for generous supporting of our research. Many thanks to all those who were involved in this work.

## Notes and references

- (a) F. Y. C. Boey, X.-L. Song, C.-Y. Yue and Q.-S. Zhao, *J. Polym. Sci., Part A: Polym. Chem.*, 2000, **38**, 907; (b) Y. Xiong and F. Y. C. Boey, *J. Appl. Polym. Sci.*, 2003, **90**, 2229; (c) X. Hu, J. Zhang, C.-Y. Yue and Q.-S. Zhao, *High Perform. Polym.*, 2000, **12**, 419.
- J. King, M. Chaudhari and S. Zahir, *29th National SAMPE Symposium*, 1984, vol. 29, p. 392.
- H. Stenzenberger, P. König, M. Herzog and W. Romer, *18th SAMPE Tech Conference*, 1986, vol. 18, p. 500.

- 4 (a) X.-H. Xiong, P. Chen, Q. Yu, N.-B. Zhu and J.-F. Li, *Polym. Int.*, 2010, **59**, 1665; (b) X.-H. Xiong, P. Chen, Q. Yu and J.-X. Zhang, *Polym. Eng. Sci.*, 2011, **51**, 1599.
- 5 L.-R. Bao and A.-F. Yee, *Polymer*, 2002, **43**, 3987.
- 6 K.-F. Lin, J.-S. Lin and C.-H. Cheng, *J. Polym. Sci., Part A: Polym. Chem.*, 1997, **35**, 2469.
- 7 Q. Fang, X.-M. Ding, X.-Y. Wu and L.-X. Jiang, *Polymer*, 2001, **42**, 7595.
- 8 R.-P. Chartoff, J. Cho and P. S. Carlin, *Polym. Eng. Sci.*, 1991, **31**, 563.
- 9 M. Abbate, E. Martuscelli, P. Musto and G. Ragosta, *J. Appl. Polym. Sci.*, 1997, **65**, 979.
- 10 A. Gopala, H. Wu, F. Harris and P. Heiden, *J. Appl. Polym. Sci.*, 1998, **69**, 469.
- 11 F.-W. Huang, Z.-X. Rong, X.-N. Shen and F.-R. Huang, *Polym. Eng. Sci.*, 2008, **48**, 1022.
- 12 T. Iijima, N. Hayashi, T. Oyama and M. Tomoi, *Polym. Int.*, 2004, **53**, 1417.
- 13 M. Shaua, P. Tsaib, W. Tenga and H. Wenhsiag, *Eur. Polym. J.*, 2006, **42**, 1899.
- 14 W.-J. Shu, L.-H. Perng and W.-K. Chin, *J. Appl. Polym. Sci.*, 2002, **83**, 1919.
- 15 Y.-L. Liu, R.-J. Jeng and Y.-S. Chiu, *J. Polym. Sci., Part A: Polym. Chem.*, 2001, **39**, 1716.
- 16 (a) H.-Y. Tang, N.-H. Song, X.-F. Chen and Q.-F. Zhou, *J. Appl. Polym. Sci.*, 2008, **109**, 190; (b) H.-Y. Tang, N.-H. Song, Z.-H. Gao and Q.-F. Zhou, *Polymer*, 2007, **48**, 129.
- 17 J.-C. Milano, S. Mekkid and J.-L. Vernet, *Eur. Polym. J.*, 1997, **33**, 1333.
- 18 (a) C.-S. Wang and C.-H. Lin, *Polymer*, 1999, **40**, 5665; (b) C.-S. Wang and H.-J. Hwang, *Polymer*, 1996, **37**, 499; (c) C.-S. Wang and H.-J. Hwang, *J. Polym. Sci., Part A: Polym. Chem.*, 1996, **34**, 1493; (d) H.-G. Hwang, C.-H. Lin and C.-S. Wang, *Polym. Int.*, 2006, **55**, 1341.
- 19 D. G. Liaw, D. C. H. Liu, B. Y. Liaw and T. I. Ho, *J. Appl. Polym. Sci.*, 1999, **73**, 279.
- 20 Z.-Q. Hu, S.-J. Li and C.-H. Zhang, *J. Appl. Polym. Sci.*, 2008, **107**, 1288.
- 21 S. H. Hsiao and C.-H. Yu, *J. Polym. Sci., Part A: Polym. Chem.*, 1998, **36**, 1847.
- 22 M. D. Iosip, M. Bruma, I. Ronova and P. Muller, *Eur. Polym. J.*, 2003, **39**, 2011.
- 23 (a) F. A. Bottino, G. D. Pasquale and A. Pollicino, *Macromol. Rapid Commun.*, 1999, **20**, 405; (b) F. A. Bottino, G. D. Pasquale and P. Iannelli, *Macromolecules*, 2001, **34**, 33.
- 24 C. Hamciuc, E. Hamciuc and M. Bruma, *Polymer*, 2005, **46**, 5851.
- 25 S. L. Gaonkar, K. M. L. Rai and B. Prabhuswamy, *Eur. J. Med. Chem.*, 2006, **41**, 841.
- 26 (a) I. K. Varam, G. M. Fohlen and J. A. Parker, *J. Polym. Sci., Polym. Chem. Ed.*, 1982, **20**, 283; (b) I. K. Varma and R. J. Tiwari, *J. Therm. Anal.*, 1987, **32**, 1023.
- 27 M. F. Grenier-Loustalot and L. D. Cunha, *Polymer*, 1997, **38**, 6303.